processes

MDPI

Article

Power Quality Disturbance Identification Method Based on Improved CEEMDAN-HT-ELM Model

Ke Liu [1], Jun Han [1], Song Chen [2,*], Liang Ruan [2], Yutong Liu [1] and Yang Wang [2]

[1] Electric Power Research Institute of State Grid Qinghai Power Grid Corporation, Xining 810008, China; liuke19882024@163.com (K.L.); hanjun19942024@163.com (J.H.); qhkeji2024@163.com (Y.L.)
[2] College of Electrical Engineering, Sichuan University, Chengdu 610065, China; ruan_liang@stu.scu.edu.cn (L.R.); fwang@scu.edu.cn (Y.W.)
* Correspondence: chen_song@stu.scu.edu.cn

Abstract: The issue of power quality disturbances in modern power systems has become increasingly complex and severe, with multiple disturbances occurring simultaneously, leading to a decrease in the recognition accuracy of traditional algorithms. This paper proposes a composite power quality disturbance identification method based on the integration of improved Complementary Ensemble Empirical Mode Decomposition (CEEMDAN), Hilbert Transform (HT), and Extreme Learning Machine (ELM). Addressing the limitations of traditional signal processing techniques in handling nonlinear and non-stationary signals, this study first preprocesses the collected initial power quality signals using the improved CEEMDAN method to reduce modal aliasing and spurious components, thereby enabling a more precise decomposition of noisy signals into multiple Intrinsic Mode Functions (IMFs). Subsequently, the HT is utilized to conduct a thorough analysis of the reconstructed signals, extracting their time-amplitude information and instantaneous frequency characteristics. This feature information provides a rich data foundation for subsequent classification and identification. On this basis, an improved ELM is introduced as the classifier, leveraging its powerful nonlinear mapping capabilities and fast learning speed to perform pattern recognition on the extracted features, achieving accurate identification of composite power quality disturbances. To validate the effectiveness and practicality of the proposed method, a simulation experiment is designed. Upon examination, the approach introduced in this study retains a fault diagnosis accuracy exceeding 95%, even amidst significant noise disturbances. In contrast to conventional techniques, such as Convolutional Neural Network (CNN) and Support Vector Machine (SVM), this method achieves an accuracy enhancement of up to 5%. Following optimization via the Particle Swarm Optimization (PSO) algorithm, the model's accuracy is boosted by 3.6%, showcasing its favorable adaptability.

Keywords: power quality disturbances; complementary ensemble empirical mode decomposition (CEEMDAN); Hilbert transform (HT); extreme learning machine (ELM)

check for updates

Academic Editors: Dimitris Ipsakis and Andreas Yiotis

Received: 23 October 2024
Revised: 10 December 2024
Accepted: 11 December 2024
Published: 7 January 2025

Citation: Liu, K.; Han, J.; Chen, S.; Ruan, L.; Liu, Y.; Wang, Y. Power Quality Disturbance Identification Method Based on Improved CEEMDAN-HT-ELM Model. *Processes* **2025**, *13*, 137. https://doi.org/10.3390/pr13010137

Copyright: © 2025 by the authors. Licensee MDPI, Basel, Switzerland. This article is an open access article distributed under the terms and conditions of the Creative Commons Attribution (CC BY) license (https://creativecommons.org/licenses/by/4.0/).

1. Introduction

The stability and purity of power quality are crucial to the normal operation of power systems and the stability of electrical equipment. Power quality issues can manifest as voltage instability, frequency fluctuations, increased harmonic content, and the presence of current asymmetry [1]. Among these, voltage stability is directly related to the normal operation of electrical devices, frequency stability is vital for the operation of synchronous equipment, and harmonic content and current asymmetry can lead to equipment damage

and reduced system energy efficiency [2]. The root causes of power quality issues include nonlinear loads, the integration of renewable energy sources, and equipment failures [3]. Harmonics and current asymmetry generated by nonlinear loads are common problems, while the instability of renewable energy sources also poses challenges to power quality. Equipment failures may cause voltage sags, voltage swells, and other issues, further affecting the stability of power systems [4]. Maintaining good power quality requires the integrated application of traditional and novel power quality improvement technologies, including power electronic devices, static reactive power compensation devices, intelligent dispatching and control systems, and more. Comprehensive analysis and monitoring can promptly identify and resolve power quality issues, safeguarding the normal operation of power systems, improving energy utilization efficiency, extending equipment lifespan, and ensuring the safe and stable operation of user equipment [5]. Therefore, maintaining power quality is not only a fundamental requirement for the operation of power systems but also a critical aspect of promoting sustainable energy development.

The detection of harmonics and inter-harmonics is the foundation and prerequisite for harmonic analysis and management. At present, domestic and foreign scholars have achieved remarkable results in the research of harmonic detection, while inter-harmonic detection remains a research difficulty and hotspot in power grid power quality due to its high demand for algorithm resolution [6]. Fourier Transform is a classic algorithm for spectrum analysis, known for its practicality, speed, and efficiency. Several widely used Fourier Transform algorithms include Fast Fourier Transform (FFT) [7], Discrete Fourier Transform (DFT) [8], and Short-Time Fourier Transform (STFT) [9]. However, Fourier Transform algorithms require synchronous sampling, which is practically impossible to achieve strictly. To approach synchronous sampling and reduce synchronization errors, two main methods are employed: hardware synchronization and software synchronization [10,11]. Hardware synchronization achieves synchronous sampling through the addition of phase-locked loop hardware circuits, which are widely used in practical applications. Scholars have also proposed improved phase-locked loops and digital phase-locked loops. Conventional software synchronization methods first measure the signal period, divide it by the number of sampling points within that period to obtain the sampling interval, and finally achieve synchronous sampling through timed interrupts [12]. Additionally, dual-rate sampling and optimized selection of sampling points have also been proposed to achieve synchronous sampling. Non-synchronous sampling can easily lead to spectral leakage and the fence effect with Fourier Transform, affecting the accuracy of spectrum detection [13]. To reduce errors caused by spectral leakage and the fence effect due to non-synchronous sampling, some scholars have proposed windowed interpolation algorithms and were the first to introduce the idea of windowed interpolation into harmonic detection [14]. Windowing can reduce spectral leakage, while interpolation can eliminate the fence effect, making this algorithm the most popular solution in practical engineering. A window function with a narrower main lobe width and lower sidelobe amplitude will have better time-domain characteristics. Furthermore, wavelet transform analysis is also widely used in harmonic detection. The principle involves decomposing the measured signal into different frequency bands using wavelet decomposition according to a certain scale, and then reconstructing the original signal based on these frequency bands [15]. Due to its excellent time-domain and frequency-domain local characteristics, wavelet transform achieves adaptive changes in the time–frequency window, overcoming the fixed-time–frequency window width and low-resolution drawbacks of Fourier Transform. Reference [16] proposes the Mallat harmonic detection method, which combines multi-resolution analysis with wavelet transform, offering good measurement accuracy, and dynamic performance. However, the more wavelet decomposition times, the greater the error in reconstructing the signal, and multi-resolution

analysis has uneven frequency band decomposition, leading to wide high-frequency bands and narrow low-frequency bands, resulting in accurate low-frequency signal detection but significantly reduced high-frequency signal detection accuracy. Reference [17] utilizes Empirical Mode Decomposition (EMD) to extract features, but this method suffers from modal aliasing and mode overlap issues. Reference [18] adopts S transform to extract features, which can identify disturbances but is relatively complex.

The second phase in the identification process of power quality disturbance signals involves pattern recognition of the extracted feature information. Pattern recognition typically employs artificial intelligence techniques for decision-making and classification. Machine learning, as the fastest-growing branch of artificial intelligence, has become the most commonly used method for pattern recognition. Machine learning involves algorithms that enable machines to analyze and discover patterns from vast amounts of data, enabling intelligent recognition and prediction of new samples. Currently, machine learning has undergone two major stages of development: shallow learning and deep learning (DL). Common shallow machine learning recognition algorithms include Artificial Neural Networks (ANN) [19], Decision Trees (DT) [20], Random Forests (RF) [21], and SVM [22]. ANN is an algorithmic mathematical model that mimics the characteristics of human neural networks for distributed parallel processing. It can adjust the biases and weights between different neurons to achieve functions such as pattern recognition and function approximation. ANN excels in handling nonlinear data and is widely used in power quality disturbance identification due to its simple structure. Reference [23] proposes a composite disturbance identification method based on dual neural networks, which utilizes an adaptive linear network to obtain feature vectors for detecting and classifying signal disturbances such as surges, harmonics, and power outages. Reference [24] combines ANN with HT, using EMD to decompose signals into IMFs and extract instantaneous amplitude and spectral information to classify transient signals. In practical applications of ANN, a large number of samples are often required, and the training time can be lengthy, limiting its application in power quality disturbance identification. DT mimics human logical thinking to establish rules and achieve classification, characterized by a simple structure and ease of implementation. Reference [25] constructs a rule-based DT classification method based on features extracted using FFT transform, dynamic measure algorithm, and S transform. Reference [26] extracts classification features based on the curve differences obtained after HT transformation and adaptively determines feature thresholds through the construction of a classification DT model. However, DT suffers from issues such as slow convergence, high sensitivity to noise, and high dependence on training samples. RF is a popular learning algorithm based on DT in recent years. RF is a large ensemble classifier composed of multiple tree-structured DT classifiers, combining the random subspace algorithm with the Bagging algorithm [27]. Its basic principle is to improve prediction and classification accuracy through the combination of multiple DTs. Reference [28] achieves a high accuracy in power quality disturbance signal identification by combining an improved S transform with the RF algorithm. However, RF's drawback lies in the significant time and space required for training when there are too many DTs, limiting its development in the field of power quality disturbance identification. SVM is a supervised learning method for nonlinear system modeling and pattern recognition [29]. It overcomes ANN's shortcomings of slow convergence and local optimal solutions, offering advantages such as good global optimization, strong generalization ability, and short training time, making it suitable for small sample classification problems. Reference [30] combines an improved wavelet transform with SVM to construct an integrated model for power quality disturbance identification. Reference [31] combines the Genetic Algorithm with SVM to build an identification model, achieving promising experimental results.

Despite the progress made in the aforementioned research, several issues and challenges still persist:

(1) When faced with multiple power quality disturbances occurring simultaneously, the recognition accuracy of traditional algorithms drops significantly. Furthermore, existing signal processing techniques struggle to fully extract the time–frequency characteristics underlying complex, nonlinear, and non-stationary power signals, making it particularly challenging to accurately identify composite power quality disturbances.

(2) Difficulty in Processing Nonlinear and Non-Stationary Signals: Since power quality signals are typically nonlinear and non-stationary, this complicates the effective decomposition and feature extraction of the signals. Traditional signal processing methods may not be able to accurately decompose noisy signals into multiple IMFs, thereby affecting the accuracy of subsequent classification and identification.

To address the aforementioned issues, this paper proposes a power quality disturbance identification method based on an improved CEEMDAN-HT-ELM model. The key innovations of this paper can be summarized as follows:

(1) This paper proposes a hybrid power quality disturbance identification method based on improved CEEMDAN, HT, and ELM. This method can effectively handle nonlinear and non-stationary signals, enhancing the identification accuracy.

(2) This paper introduces an improved ELM as the classifier, leveraging its powerful nonlinear mapping capability and fast learning speed for pattern recognition of extracted features, achieving accurate identification of hybrid power quality disturbances.

The organization of the full paper is as follows: Sections 2 and 3 constitute the methodology, which introduces in detail the denoising decomposition algorithm and the power disturbance identification model. Section 4 presents a case study, demonstrating the feasibility and effectiveness of the method proposed in this paper. Finally, Section 5 summarizes the entire paper.

2. CEEMDAN Algorithm Principle and Mathematical Model

2.1. Basic Principles

First, the noisy signal containing power quality disturbances is decomposed into several IMFs using the CEEMDAN algorithm. The process is as follows:

According to Equation (1), the signal $X(t)$ is constructed as [5]:

$$X(t) = x(t) + \varepsilon_0 w_i(t) \tag{1}$$

where $x(t)$ represents the original signal; $X(t)$ represents the signal with white noise added; ε_0 is the amplitude coefficient of the white noise; $\omega_i(t)$ represents the white noise.

By applying EMD to the signal $X(t)$, the first-order IMF component and the corresponding residue component can be obtained [7], as shown in Equations (2) and (3):

$$IMF_1(n) = \frac{1}{N}\sum_{i=1}^{N} IMF_1^i(n) \tag{2}$$

$$r_1(n) = x(n) - IMF_1(n) \tag{3}$$

Here, N represents the number of modal components generated, and n is an index variable used to iterate through or index all data samples of the first intrinsic mode function. IMF_1^i represents the intrinsic mode components obtained through CEEMDAN decomposition, and Equation (3) is used to calculate the residual after removing the first modal

component. The residue component $r_1(n)$ obtained from Equation (3) is then decomposed again to yield the second-order IMF component [11], as shown in Equation (4):

$$IMF_2(n) = \frac{1}{N}\sum_{i=1}^{N} E_1\{r_1(n) + \varepsilon_1 E_1[w_i(n)]\} \tag{4}$$

In the equation, $E_j(\cdot)$ represents the j-th order component. Following this process, the j-th residual signal component can be expressed as [5]:

$$r_j(n) = r_{j-1}(n) - IMF_n(n) \tag{5}$$

The $(j + 1)$-th order IMF component can be expressed as:

$$IMF_{j+1}(n) = \frac{1}{N}\sum_{i=1}^{N} E_1\{r_{j+1}(n) + \varepsilon_j E_j[w_i(n)]\} \tag{6}$$

By repeating the above steps until the signal can no longer be decomposed further, the algorithm stops, yielding a total of the j-th IMF components. Using an IMF component selection criterion, the decomposed IMF components are categorized into signal IMF components, aliased IMF components, and noise IMF components. The original signal after decomposition can be represented as:

$$x(n) = r(n) + \sum_{j=1}^{k} IMF_j + \sum_{j=k+1}^{m} IMF_j + \sum_{j=m+1}^{n} IMF_j \tag{7}$$

In the above equation, $r(n)$ represents the final residual component; $\sum_{j=1}^{k} IMF_j$ represents the signal IMF components; $\sum_{j=k+1}^{m} IMF_j$ represents the aliased IMF components; and $\sum_{j=m+1}^{n} IMF_j$ represents the noise IMF components.

Given the different frequency ranges associated with the aliased IMF components and noise IMF components, a combined denoising approach is utilized, leveraging the advantages of different denoising methods. The final denoised signal can be expressed as:

$$x(n)^{\Delta} = r(n) + \sum_{j=1}^{k} IMF_j + \sum_{j=k+1}^{m} IMF_j^{\Delta} + \sum_{j=m+1}^{n} IMF_j^{\Delta} \tag{8}$$

where $\sum_{j=k+1}^{m} IMF_j^{\Delta}$ represents the denoised aliased IMF components, and $\sum_{j=m+1}^{n} IMF_j^{\Delta}$ represents the denoised noise IMF components.

2.2. IMF Component Selection Criterion

In order to achieve better denoising results, this paper attempts to introduce the Renyi's entropy-based distance method to subdivide the IMF components obtained from CEEMDAN decomposition into three categories: signal IMF components, aliased IMF components, and noise IMF components. The Probability Density Function (PDF) contains complete characteristic information of a signal. This paper employs the kernel-smoothed PDF method to calculate the PDF of each IMF component and the original signal separately. An improved Renyi's distance is then used to evaluate the similarity between the PDF of

each IMF component and the PDF of the original signal. For two sets $M_i = \{m_1, m_2, \ldots, m_k\}$ and $N_i = \{n_1, n_2, \ldots, n_k\}$, the improved Renyi's distance between these two sets is defined as:

$$D(M_i, N_i) = \frac{1}{k}\sum_{j=1}^{k}\frac{|m_i - n_i|}{|m_i|} \tag{9}$$

In the above equation, a smaller value of $D(M_i, N_i)$ indicates a higher similarity between the two sets. It is generally believed that noise is primarily distributed in the high-frequency portion of the signal represented by the low-order IMF components. After the minimum value point of the improved Renyi's distance is reached, as the order of the IMF components increases, the noise contained in the IMF components rapidly decreases. In all, the improved CEEMDAN method is used to preprocess the collected initial power quality signals. The entire process can be described through Equations (1)–(9). Through Equations (1)–(8), the initial noise signal is decomposed into multiple IMFs, and Equation (9) is further applied to reduce modal mixing and artifact components. In addition to the distance method based on Rényi entropy, there are various other methods that can be used for the subdivision of IMF components, such as those based on mutual information, correlation coefficient, and Euclidean distance. Rényi entropy is capable of quantifying the uncertainty or complexity of signals and exhibits high sensitivity to minute changes in signals. In the classification of power quality disturbances, IMF components of different disturbance types possess distinct complexity characteristics, and the distance method based on Rényi entropy can effectively capture these differences, thereby achieving more precise subdivision. Furthermore, this method possesses a certain degree of robustness against noise, capable of suppressing noise interference to a certain extent and enhancing the accuracy of classification. However, the distance method based on Rényi entropy involves relatively complex calculations, increasing the computational burden of the algorithm. Therefore, in situations where computational resources are limited, a balance needs to be struck between computational complexity and classification accuracy.

3. Power Quality Disturbance Identification Model Based on Hilbert Transform and Improved Extreme Learning Machine

3.1. Introduction to Hilbert Transform

Given a random signal $z(t)$ in the real domain, its HT expression [4] is:

$$y(t) = H[z(t)] = \frac{1}{\pi}\int_{-\infty}^{+\infty}\frac{z(\tau)}{t-\tau}d\tau \tag{10}$$

The inverse transform of the above Equation (10) can be expressed as:

$$z(t) = H^{-1}(y(t)) = -\frac{1}{\pi}\int_{-\infty}^{+\infty}\frac{y(\tau)}{t-\tau}d\tau \tag{11}$$

Rewriting Equations (10) and (11) in the form of convolution gives:

$$\begin{cases} y(t) = \frac{1}{\pi t} * z(t) \\ z(t) = -\frac{1}{\pi t} * y(t) \end{cases} \tag{12}$$

Using $z(t)$ and $y(t)$, we construct a complex-valued function $s(t)$ as:

$$s(t) = z(t) + jy(t) = z(t) + jH[z(t)] \tag{13}$$

Denoting $s(t) = A[z(t)]$, then the following equation holds:

$$A[z(t)] = z(t) + jH[z(t)] = a(t)e^{j\theta(t)} \tag{14}$$

$$a(t) = \sqrt{z^2(t) + y^2(t)} = \sqrt{z^2(t) + H^2[z(t)]} \tag{15}$$

$$\theta(t) = \arctan\frac{y(t)}{z(t)} = \arctan\frac{H[z(t)]}{z(t)} \tag{16}$$

In the Equations (14) and (16), $a(t)$ and $\theta(t)$ represent the instantaneous amplitude and instantaneous phase of the random signal function $z(t)$ using Equation (12), respectively. The frequency can be obtained by differentiating the phase angle, and the instantaneous frequency is given by:

$$\varpi(t) = \frac{d\theta(t)}{dt} = \frac{H'[z(t)]z(t) - H[z(t)]z'(t)}{z^2(t) + H^2[z(t)]} \tag{17}$$

Using Equations (14)–(17), the computation of the instantaneous amplitude, instantaneous phase, and instantaneous frequency of the signal $z(t)$ through HT can be completed.

3.2. Fault Diagnosis Model Based on Extreme Learning Machine

The ELM algorithm is a network algorithm proposed based on feedforward neural networks [12,16]. It is a typical single-hidden layer feedforward neural network, with a structure as shown in Figure 1. The initial power quality signals are preprocessed using the improved CEEMDAN method to reduce modal aliasing and spurious components, thereby enabling a more precise decomposition of the signals into multiple IMF. The HT is then utilized to conduct an in-depth analysis of the reconstructed IMF signals, extracting their time–amplitude information and instantaneous frequency characteristics. This extracted feature information, including time–amplitude information and instantaneous frequency characteristics, constitutes the input for the ELM. The output is the encoded type of power quality disturbance; for example, harmonic disturbances are encoded as 1, voltage sag disturbances as 2, and so on.

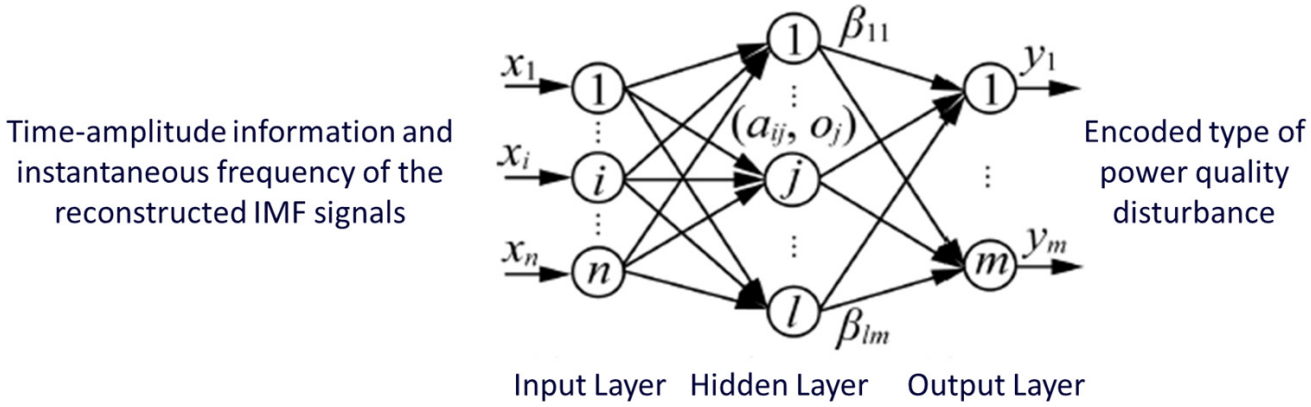


Figure 1. Schematic Diagram of ELM Structure Framework.

The ELM algorithm architecture consists of three layers of neurons: the input layer, the hidden layer, and the output layer. The neurons within each layer are fully connected. The input layer has n neurons, the hidden layer has l neurons, and the output layer has m neurons. a_{ij} represents the connection weight between the input layer and the hidden layer, o_j represents the threshold of each hidden layer neuron, and β_{ij} represents the connection weight between the hidden layer and the output layer.

Assuming $g(x)$ is the activation function of the hidden layer [13], the output is expressed as shown in Equation (18), where $i = 1, 2, \ldots, n$; $j = 1, 2, \ldots, l$; $k = 1, 2, \ldots, m$.

$$y_k = \sum_{i}^{n} \beta_{jk} g(a_{ij} x_i + o_j) \tag{18}$$

Let H be the output matrix of the hidden layer, as shown in Equation (19).

$$H(a_1, a_2, \ldots, a_l, o_1, o_2, \ldots, o_l, x_1, x_2, \ldots, x_n) = \begin{bmatrix} g(a_1 x_1 + o_1) & \cdots & g(a_l x_1 + o_l) \\ \cdots & \cdots & \cdots \\ g(a_1 x_n + o_1) & \cdots & g(a_l x_n + o_l) \end{bmatrix}_{n \times l} \tag{19}$$

Given the output matrix as Y, we have $H\beta = YT$, leading to Equation (8).

$$\beta = H^{-1} Y^T \tag{20}$$

In the ELM algorithm, the connection weights between the input layer and the hidden layer are randomly generated, and the thresholds of the hidden layer neurons are also randomly set. During training, after selecting the activation function, only the number of hidden layer neurons needs to be determined, and then the connection weight matrix β_{ij} between the hidden layer and the output layer can be calculated. Through the weight matrix β_{ij}, untrained data can be further tested, offering advantages such as fast learning speed and strong generalization performance. However, there are also certain issues. The random generation of connection weights between the input layer and the hidden layer, as well as the thresholds of the hidden layer neurons, can affect the training results of the ELM algorithm each time, which in turn affects its generalization performance.

$$\beta = (H^T H)^{-1} H^T Y^T \tag{21}$$

$$\beta = (H^T H + \lambda I)^{-1} H^T Y^T \tag{22}$$

The random generation of connection weights between the input layer and the hidden layer, as well as the thresholds of the hidden layer neurons, can lead to uncertainty in the calculation results, making it difficult to achieve the desired results through just one or a few calculations. To reduce the error caused by random data, the PSO algorithm is used to iteratively optimize the input connection weights and thresholds of the ELM algorithm with regularization parameters [32,33]. The specific steps are as follows:

1. Establish training and testing samples based on the extracted signal features.
2. Introduce regularization parameters and perform optimal parameter setting.
3. Set the input connection weights and hidden layer neuron thresholds of the Regularized ELM (RELM) algorithm as particles, and determine the particle length.
4. Configure the relevant parameters of the PSO algorithm, including speed update parameters, iteration count, population size, maximum and minimum speed values, etc.
5. Use the root mean square error (RMSE) value of the initialized particles in the training samples as the fitness value for each particle. Continuously iterate and select the larger fitness value as the new individual best and global best.
6. Stop the iteration when the RMSE value meets the specified condition or the maximum iteration count is reached. The corresponding particle at this point represents the optimal input connection weights and hidden layer neuron thresholds to be found.

7. Use the optimal parameters to assign values to the input layer and hidden layer of the RELM algorithm, thereby obtaining the optimal RELM algorithm parameter model. This model can then be used to classify and identify power quality disturbance signals.

To gain a better understanding, the flowchart of the proposed method is given in Figure 2. With the construction of digital power systems, the widely installed smart meters and fault recording devices can provide data for the ELM training set. The fault voltage waveforms recorded by the fault recording devices can be extracted and analyzed in real-time by the control center. These data are representative and authentic, reflecting various possible disturbance scenarios in the power system. The timing for retraining the ELM model depends on the following three factors: 1. Environmental changes: If the operating environment of the power system changes (such as the introduction of new loads, changes in grid structure, etc.), the ELM may need to be retrained to adapt to new disturbance characteristics. 2. Performance decline: If the performance of the ELM in practical applications declines to a certain extent (e.g., accuracy falls below a certain threshold), retraining is necessary to enhance its performance. 3. Data updates: As new data are continuously collected and processed, the training set can be periodically updated, and the ELM retrained to capture the latest disturbance characteristics and improve the model's generalization ability. Retraining of the model is required when any of the above three situations occur.

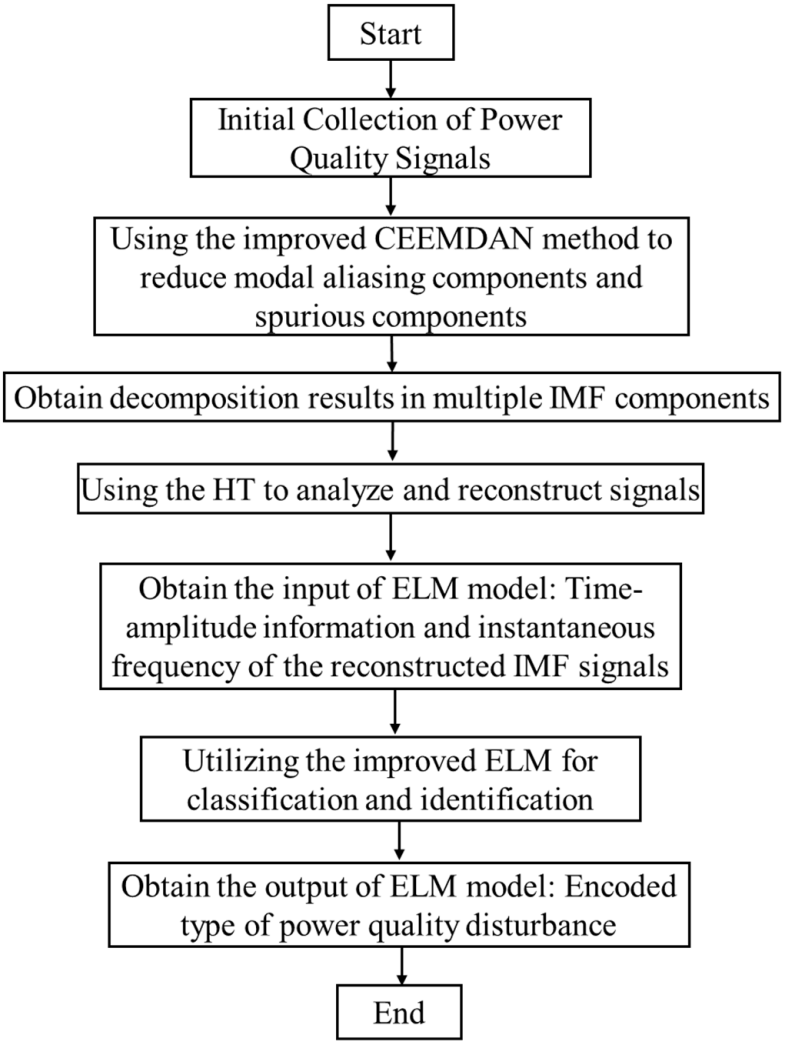


Figure 2. The flowchart of the proposed method.

4. Case Study with Discussions

In the process of identifying power quality disturbance signals, the collected voltage signals are selected for analysis and diagnosis. Issues related to power quality, such as voltage fluctuations, voltage sags, voltage swells, voltage interruptions, and harmonics, are directly reflected in the voltage signals. These disturbance types were chosen and emphasized based primarily on their prevalence in power systems and their impact on system stability and equipment operation. Voltage fluctuations refer to variations in voltage levels around its average value over a period of time. Such fluctuations can lead to decreased equipment performance or even damage. Harmonics cause distortion in voltage and current, affecting the normal operation of power equipment, shortening equipment lifespan, and reducing the stability and efficiency of power systems. Voltage sags and swells may cause sensitive equipment to shut down or fail to restart, significantly impacting industrial production, commercial operations, and residential life. Voltage interruptions can result in equipment shutdown, data loss, and other severe consequences, posing a threat to the reliability and stability of power systems. It should be noted that, within the context of this paper, the primary focus is on harmonics. Harmonics are ubiquitous in power systems and are becoming increasingly severe with the increase in nonlinear loads. The monitoring of harmonics requires high-precision measurement equipment and professional analysis techniques. The mitigation of harmonics necessitates comprehensive consideration of factors such as grid structure, load characteristics, and filtering devices, posing significant challenges. In other words, if the method proposed in this paper can accurately identify harmonics, it can also achieve efficient identification and classification of other types of disturbances. Therefore, by monitoring and analyzing these voltage signals, one can intuitively understand the status of power quality. In power systems, voltage signals are generally easy to collect using sensors or measurement equipment. Furthermore, the processing and analysis of voltage signals are relatively straightforward, allowing for feature extraction and pattern recognition using existing signal processing techniques and algorithms. Power quality disturbances often lead to equipment failures or performance degradation. There is a close relationship between changes in voltage signals and these failures. For instance, voltage sags may cause motors to shut down or fail to restart, while voltage interruptions may result in equipment shutdown or data loss. By analyzing voltage signals, these potential issues can be promptly identified, and corresponding measures can be taken for prevention or repair.

4.1. Effectiveness Validation of the CEEMDAN Algorithm

In the identification of power quality disturbances in electric power systems, harmonics are considered one of the most complex and challenging disturbances to extract features from. The harmonic data utilized in this Section were collected from smart meters of State Grid Jiangsu Electric Power Company in real-world scenarios, with a total sample size of 36,000. The relevant data have been published on the open-source data website CSDN, and researchers can download them via the link [34]. The model of the smart meter employed here is APM510 which is produced by China Jiangsu Ankui Electric Appliance Manufacturing Co., Ltd., as shown in Figure 3. It can accurately measure electrical parameters such as current, voltage, and power factor. Harmonics not only consist of frequency components that are integer multiples of the fundamental frequency but can also occur simultaneously in multiple forms, forming a complex harmonic spectrum. Furthermore, the amplitude, phase, and other parameters of harmonics may vary over time, adding to their complexity. In power systems, multiple harmonics may coexist and interact with each other, making it even more difficult to extract the features of a single harmonic. Additionally, there may be overlapping or similar frequencies and amplitudes among different harmonics, fur-

ther complicating feature extraction. To address complex harmonic signals, the proposed method and the traditional Ensemble Empirical Mode decomposition (EEMD) algorithm are compared and illustrated in Figures 4 and 5 below, respectively.



Product Appearance

Model	APM510
Performance	It can accurately measure electrical parameters such as current, voltage, and power factor, and supports multiple communication protocols like RS485 and Ethernet, which facilitates connection with remote systems and data transmission, enabling real-time data transmission and calculation.
Applicable Types of Disturbance Analysis	Harmonics, Inter-harmonics, Flicker, and Voltage Fluctuations

Figure 3. Structural Diagram and Related Introduction of the Smart Meter.

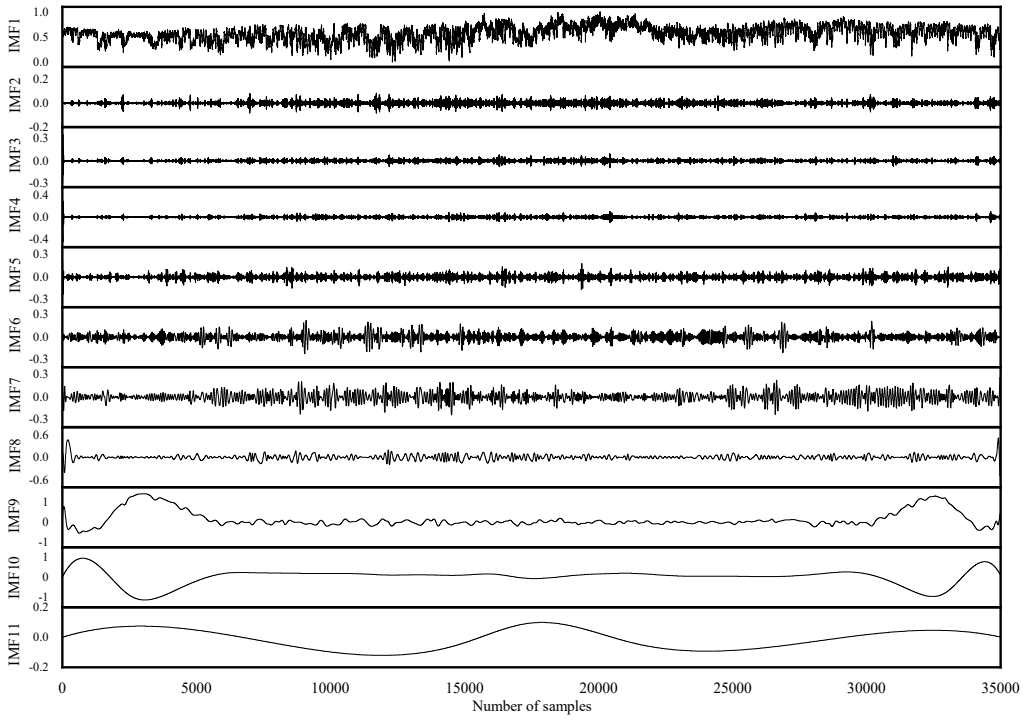


Figure 4. The decomposition results of harmonic signals obtained through the CEEMDAN algorithm.

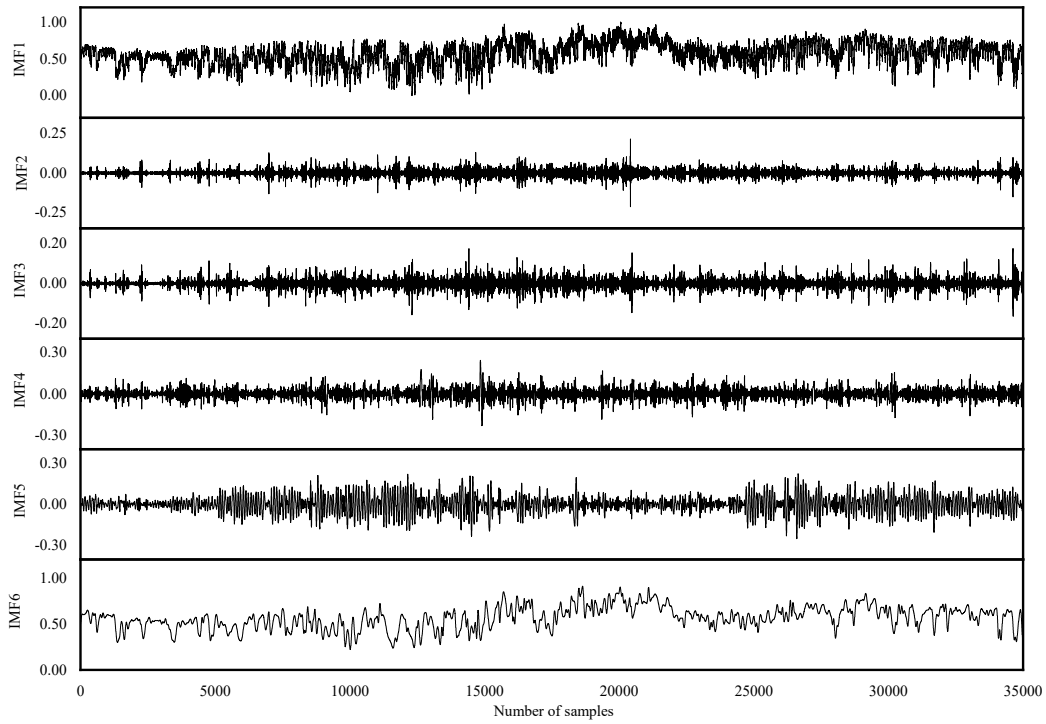


Figure 5. The decomposition results of harmonic signals obtained through the EEMD algorithm.

Upon observing Figures 4 and 5, it becomes evident that the CEEMDAN algorithm, during the decomposition process, not only adds Gaussian white noise to the original signal but also adaptively incorporates specific noise based on the outcome of the previous decomposition stage at each iteration. This adaptive noise addition approach facilitates a more detailed revelation of different frequency components within the signal, resulting in a greater number of decomposed components. While the EEMD algorithm addresses the mode mixing issue in EMD by introducing white noise, the noise added is global and remains constant throughout the entire decomposition process. In contrast, CEEMDAN further mitigates mode mixing by incorporating noise related to the previous stage at each step, leading to a finer decomposition outcome with potentially more components. When decomposing harmonic signals, the 11 IMF components obtained each represent the time evolution of different frequency components within the signal. Generally, the first few IMF components (such as IMF1, IMF2, etc.) represent high-frequency components or noise in the signal. These components capture the rapidly changing parts of the data, which may include noise, interference, or other high-frequency characteristics within the signal. As the sequence number of the IMF components increases, the frequencies gradually decrease. The intermediate IMF components (such as IMF3 to IMF6, etc.) typically represent medium-frequency components in the signal. These components reflect the fluctuation characteristics of the signal within the medium-frequency range. The later IMF components (such as IMF7 to IMF11, etc.) represent low-frequency components in the signal. These components capture the slower-changing parts of the signal, which may include trend components or very low-frequency fluctuations.

In this paper, two indicators—modal aliasing degree and reconstruction error are selected to quantitatively assess the effectiveness of the method. Through analysis, the modal aliasing degree and reconstruction error of the strategy proposed in this paper are 0.0028 and 1.78%, respectively, while those of the EEMD strategy are 0.0108 and 4.59%. This suggests that the IMF components decomposed using the strategy proposed in this paper can more accurately reflect the different frequency components in the signal and preserve more complete original signal information. Due to the use of adaptive noise addition

and a more refined decomposition strategy, the CEEMDAN algorithm typically achieves higher decomposition accuracy. This enhances the precision in identifying and extracting characteristic information from power quality harmonic disturbance signals. Compared to EEMD, CEEMDAN's gradual addition and removal of noise during decomposition more effectively suppresses the influence of noise on the decomposition results, which is crucial for improving the accuracy of harmonic disturbance signal analysis.

Not only is the CEEMDAN algorithm suitable for decomposing power quality harmonic disturbance signals, but it is also widely applied in signal processing tasks across various fields. Its robust signal decomposition capabilities and broad applicability make it a significant player in the signal processing domain. The multiple IMFs obtained through CEEMDAN decomposition represent different frequency scales within the signal. These components can be further utilized for multi-scale analysis, providing a more comprehensive understanding of signal characteristics and variation patterns. The large number of relatively independent IMFs from CEEMDAN decomposition facilitates subsequent signal processing and analysis tasks, such as reconstruction, filtering, or feature extraction, tailored to meet diverse application requirements. The proposed method integrates advanced signal processing techniques and machine learning algorithms, enabling it to identify multiple concurrent power quality disturbance signals, including voltage fluctuations, voltage sags, voltage swells, voltage interruptions, harmonics, frequency deviations, and so on. The actual power grid structure is complex, with numerous branch lines and load variations, which complicates the propagation and distribution of harmonics. Various noise interferences exist in the power grid, such as background noise and measurement noise, which interfere with the detection and analysis of harmonics. Therefore, this paper focuses on the analysis of harmonic disturbances in power quality.

4.2. Verification of Power Quality Disturbance Identification Accuracy

Based on the RELM algorithm, five training and testing trials were conducted for each of the four different activation functions: sigmoid, sin, hardlim, and radbas. The test accuracy results are shown in Figure 6. It can be observed that among the three other activation functions, radbas achieves the highest average test accuracy, thus it was selected as the activation function. The radbas function possesses powerful nonlinear mapping capabilities. In power quality disturbance signals, which often contain complex nonlinear features, the radbas function is better able to capture these features, thereby enhancing the identification accuracy of the model.

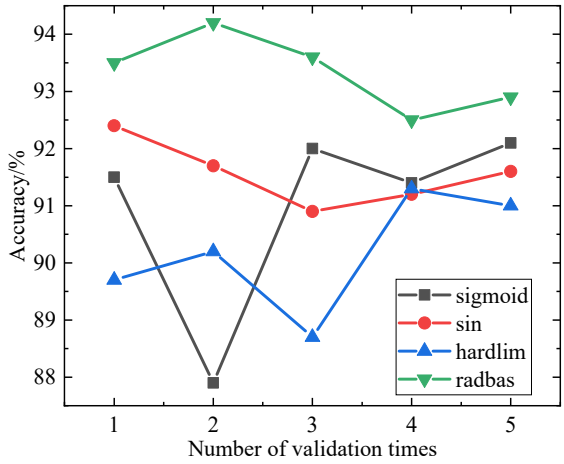


Figure 6. Verification of Accuracy with Different Activation Functions.

Compared to other activation functions, the radbas function exhibits more flexible local response characteristics. This means it can produce different output responses within different input ranges, enabling a more precise description of the local features of disturbance signals. During the training process, the radbas function may assist the ELM model in learning more generalized feature representations, enabling the model to maintain high identification accuracy even when confronted with unseen disturbance signals.

Selecting an appropriate activation function helps balance the model's complexity and generalization ability, avoiding overfitting. While traditional activation functions like sigmoid are widely used in deep learning, they may not be the optimal choice for certain specific tasks, such as power quality disturbance identification. In contrast, the radbas function may better enable the model to maintain high identification accuracy while avoiding overfitting to the training data. Through multiple training and testing trials, the advantage of the radbas function in terms of average test accuracy becomes evident. This further validates its effectiveness as an activation function for power quality disturbance identification tasks.

To further demonstrate the accuracy of the proposed method in this paper, a comparison is made with traditional ELM, SVM, and CNN models. The power quality disturbance identification accuracies are presented in Table 1 below. In this paper, the PSO algorithm is employed to iteratively refine the input connection weights, thresholds, and regularization parameters of the ELM algorithm compared to traditional methods. The total data sample consists of 200 records, obtained from fault recording devices of State Grid Jiangsu Electric Power Company in China Nanjing. The relevant data can be downloaded from an open-source data website [34]. The fault recording devices utilized in this paper are of the ZH-6 dynamic recording unit model which is produced by China Wuhan Zhongyuan Huadian Technology Co., Ltd. as illustrated in Figure 7.

In practical operation of power systems, complex situations often arise where multiple disturbances occur simultaneously. Table 2 presents the identification accuracy of the proposed method in cases where multiple disturbances occur simultaneously. The number of samples in the training set used is 150. The considered combinations of disturbance faults include the following categories:

Combination 1: Voltage sags, voltage swells, voltage interruptions, and harmonics.
Combination 2: Voltage fluctuations, voltage swells, voltage interruptions, and harmonics.
Combination 3: Voltage fluctuations, voltage sags, voltage interruptions, and harmonics.
Combination 4: Voltage fluctuations, voltage sags, voltage swells, and harmonics.

Table 1. Comparison of Power Quality Disturbance Identification Accuracies Across Different Models.

Noise/dB	Identification Accuracy/%				
	The Proposed Method	ELM Model	SVM	Transformer	CNN
5	98.7	94.3	95.6	96.8	94.9
10	97.6	93.2	95.0	95.4	93.8
15	97.2	92.4	94.8	94.2	93.6
18	95.2	90.6	93.4	93.7	91.2

Table 2. Comparison of Diagnostic Accuracy Among Different Models in Cases of Multiple Disturbances Occurring Simultaneously.

Combination	Identification Accuracy/%				
	The Proposed Method	ELM Model	SVM	Transformer	CNN
1	95.0	93.2	91.6	93.8	92.5
2	95.6	89.7	92.4	94.6	89.4
3	96.1	91.1	92.0	93.2	87.8
4	95.4	93.2	91.8	91.7	93.0



Product Appearance

Model	ZH-6 dynamic recording unit
Performance	It achieves synchronous dual storage of transient-triggered waveform data, making it suitable for substations with voltage levels of 35(66)kV and above. Field data acquisition is implemented under Linux using VXD technology.
Applicable Types of Disturbance Analysis	Short-circuit faults, system oscillations, frequency collapses, voltage collapses, harmonics

Figure 7. Structural Diagram and Related Introduction of fault recording devices.

Upon examining the table above, it is evident that the method proposed in this paper exhibits robustness and effectively copes with various noise interferences, maintaining a disturbance identification accuracy above 95%. Regularization, a common technique in machine learning, is used to prevent overfitting and enhance the model's generalization ability. In the context of ELM algorithm, incorporating a regularization parameter constrains the model's complexity, ensuring that during training, the model not only strives for high accuracy on the training set but also considers its performance on the test set or unseen data. This helps the model maintain stable performance even in the presence of noise. The ELM algorithm, based on single-hidden-layer feedforward neural networks, boasts rapid learning capabilities and strong nonlinear approximation abilities. During training, it randomly generates hidden layer node parameters and utilizes the least squares method to directly solve for the output layer weights, eliminating the need for iterative adjustment of hidden layer parameters, thereby significantly improving learning efficiency. This rapid learning capability renders ELM particularly advantageous for power quality disturbance identification and classification tasks with high real-time requirements. In this paper, the swarm size is set to 40, the number of iterations to 200, and the inertia weight is dynamically adjusted during the iteration process, gradually decreasing from 0.9 to 0.4. The cognitive learning factor and social learning factor are both set to 2. Both the PSO algorithm and the GA are widely used heuristic optimization algorithms currently. When optimizing the parameters of ELM and identifying power quality disturbance signals, the ELM model optimized by PSO exhibits higher fault diagnosis accuracy. When the number of test samples is 1000, the average diagnosis accuracies of the models optimized by PSO and GA are 98.2% and 94.6%, respectively. This is because the PSO algorithm simulates the foraging behavior of bird flocks, utilizing information sharing and collaboration among particles to search for the optimal solution. It is characterized by its ability to quickly converge to a local optimal solution and, in some cases, to escape from local optima, demonstrating good global search capabilities. When optimizing the connection weights and hidden layer neuron thresholds of the ELM model, PSO can quickly locate better parameter combinations, thereby improving the fault diagnosis accuracy of the model. In contrast, the GA simulates natural selection and genetic processes, such as crossover and mutation, to generate new individuals and optimize solutions. The GA possesses strong global search capabilities but may be time-consuming during the search process and, in some cases, prone to premature convergence, i.e., converging prematurely to a non-global optimal solution. Additionally, the parameters in the PSO algorithm (such

as inertia weight and learning factors) can be adjusted according to the characteristics of specific problems to better adapt to the optimization process. This flexibility enables PSO to more precisely control the search direction and step size when optimizing ELM model parameters, thereby finding better solutions. Although the GA also has a certain parameter adjustment space, the impact of its parameter settings on the optimization results may not be as intuitive and significant as that of PSO. When multiple disturbances occur simultaneously, their characteristics can interfere with each other, making the features of individual disturbances less obvious or difficult to distinguish. This may pose difficulties for algorithms in feature extraction, thereby reducing the subsequent classification and identification accuracy. The occurrence of multiple disturbances simultaneously implies the need to process more complex signals, which increases computational complexity and processing time. Although the Transformer model has achieved remarkable results in many fields, when dealing with issues such as power quality disturbances that exhibit complexity and nonlinearity, it may require more training data and a more complex model structure to achieve high accuracy. In contrast, the method proposed in this paper achieves high accuracy with less training data and a simpler model structure through meticulous signal preprocessing, precise feature extraction, and efficient classifier selection. Compared to the Transformer model, another significant advantage of the strategy proposed in this paper is its higher computational efficiency. When performing identification of multiple types of mixed disturbances, the computation time for the strategy proposed in this paper is 127.4 s, while the computation time for the Transformer model is 557.4 s. This is due to the complexity and high number of parameters in the Transformer model, which requires substantial computational resources for both training and inference processes. ELM is a rapid single-layer feedforward neural network training method, whose basic idea is to randomly select the weights and biases from the input layer to the hidden layer, and then directly calculate the output layer weights. When dealing with large-scale datasets or real-time fault diagnosis tasks, the ELM model may have more advantages. Considering that the dispatching time scale in power systems is generally 5 min, the method proposed in this paper can meet the needs of real-time dispatching.

Incorporating regularization parameters into the ELM algorithm significantly boosts its efficacy. This regularization component serves as a stabilizer in the objective function, facilitating a trade-off between minimizing training errors and controlling model complexity. This equilibrium aids in sustaining the model's performance stability in noisy scenarios, thus enhancing its robustness. In the realm of power quality disturbance identification and classification, practical signals frequently encounter numerous noise sources stemming from equipment, transmission lines, and other power system elements. Thanks to its robust generalization capabilities and resilience, the regularized ELM algorithm can somewhat mitigate noise interference and precisely discern types of power quality disturbances. Furthermore, the diagnostic precision of our proposed method outstrips that of conventional ELM models, SVMs, and CNNs.

While ELM algorithms excel in swift learning and nonlinear approximation, they may fall prey to overfitting without regularization, thereby undermining their performance on test sets. By fine-tuning model complexity via regularization, the ELM algorithm attains superior classification accuracy. SVMs, despite their proficiency in managing small samples and nonlinear challenges, frequently entail more intricate training procedures and demonstrate lower processing efficiency for large-scale datasets. Conversely, ELM algorithms maintain high classification accuracy while offering quicker training times and superior processing efficiency. Meanwhile, CNNs, while formidable in image processing, may not exhibit the same advantages when tackling one-dimensional time-series data, such as power quality disturbance signals, and they often necessitate extensive data and

computational resources for training. In contrast, ELM algorithms can effectively classify even with constrained resources.

4.3. Effectiveness Testing of Industrial Application

In order to further validate the effectiveness and feasibility of the method proposed in this paper within an industrial testing system, the IEEE-33-bus testing system is adopted, and its structural topology is illustrated in Figure 8 below. Four disturbance signal sources are installed at nodes 14, 20, 23, and 28 in the diagram. The noise sources can generate and superimpose different types of disturbance signals according to requirements. Figure 9 demonstrates the diagnostic accuracy under different numbers of disturbance signal sources. It should be noted that the four disturbance signal sources in Figure 6 consist of 100 sets of disturbance signals, which are derived from actual regional grid data of State Grid Jiangsu Electric Power Company. These signals can be downloaded from the open-source data website CSDN [34]. The types of faults considered include voltage sags, voltage swells, voltage interruptions, harmonics, and combinations of the aforementioned faults.

Observing Figure 9, it can be found that under the superposition of multiple types of disturbance signals, the method proposed in this paper can still maintain a diagnostic accuracy above 94.5%. Traditional algorithms have limitations when dealing with nonlinear and non-stationary signals. However, the proposed method preprocesses the initial power quality signals by introducing improved CEEMDAN, effectively reducing modal aliasing and spurious components, enabling noisy signals to be more accurately decomposed into multiple IMFs. This step significantly improves the accuracy and reliability of signal decomposition, laying a solid foundation for subsequent feature extraction and classification recognition. Secondly, the HT is utilized to conduct an in-depth analysis of the reconstructed signals, extracting their time–amplitude information and instantaneous frequency characteristics. This feature information not only contains the key characteristics of power quality disturbances but also provides abundant data support for subsequent classification and recognition. Through the transformation of HT, different types of power quality disturbance signals become more separable in the feature space. Finally, an improved ELM is introduced as the classifier, leveraging its powerful nonlinear mapping capabilities and fast learning speed to perform pattern recognition on the extracted features. The introduction of ELM not only improves the accuracy and efficiency of classification and recognition but also adapts well to the complexity of superposition of multiple types of power quality disturbance signals.

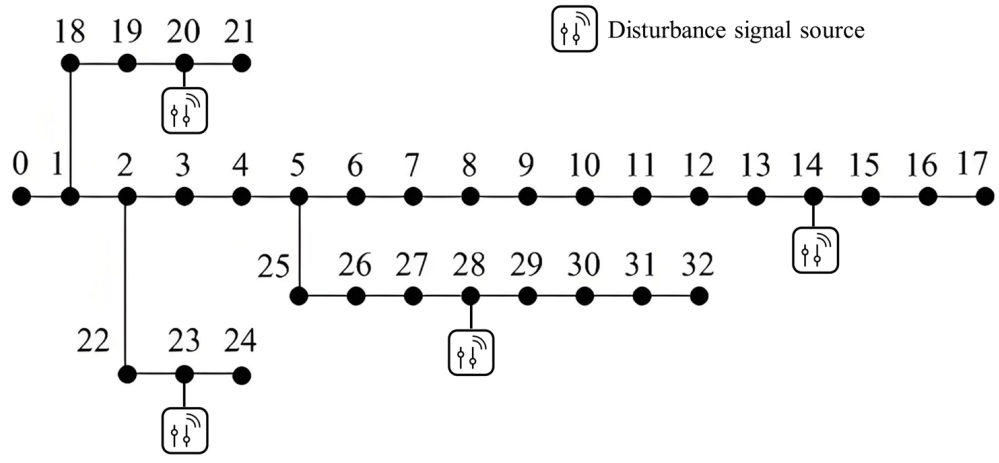


Figure 8. Structural topology of the IEEE-33-bus testing system.

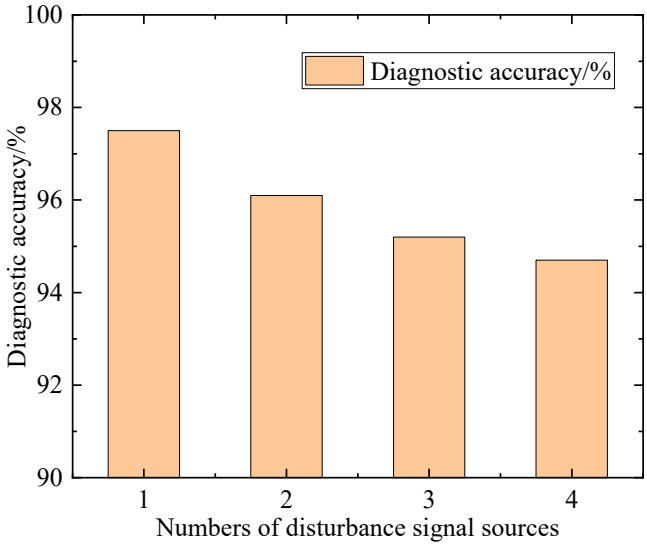


Figure 9. Diagnostic accuracy under different numbers of disturbance signal sources.

In summary, the proposed method, through improved signal preprocessing techniques, feature extraction methods, and classification recognition algorithms, effectively solves the problem of decreased recognition accuracy when traditional algorithms deal with the superposition of multiple types of power quality disturbance signals. Thus, it achieves the goal of maintaining high diagnostic accuracy even when multiple types of power quality disturbance signals are superimposed. In practical applications, this method requires high-precision sensors and data acquisition cards to capture power quality signals. Due to the involvement of complex signal processing and machine learning algorithms, high-performance computing devices (such as high-performance computers or dedicated servers) are needed to support real-time or near-real-time data processing and analysis. The physical conditions of the installation site, such as temperature, humidity, electromagnetic interference, etc., must be considered to ensure stable operation of the equipment. This adds a degree of complexity to the application and promotion. The performance of the method proposed in this paper will also be affected by parameter settings. For example, the number of decomposition layers in CEEMDAN, the choice of window function in HT, and the number of hidden layer neurons in ELM will all influence the final recognition results. Therefore, these parameters require careful tuning. Although the proposed method may achieve high recognition accuracy when dealing with complex nonlinear power quality disturbances, its computational complexity is also relatively high. Especially when processing large-scale datasets, it requires longer computation time and higher computational resources.

In the future, with the rapid development of big data and cloud computing technologies, it will become feasible to apply these technologies to the identification of power quality disturbance signals. By collecting and analyzing vast amounts of power quality data, potential patterns and characteristics of the disturbance signals can be revealed, providing data support for the optimization of identification algorithms. Meanwhile, cloud computing technology enables real-time processing and analysis of large-scale data, offering robust support for real-time monitoring and intelligent recognition in power systems.

5. Conclusions

This paper proposes an innovative hybrid power quality disturbance identification method aimed at addressing the increasingly complex and severe power quality disturbance issues in modern power systems. By integrating the improved CEEMDAN technique, HT, and an ELM classifier, the method effectively overcomes the limitations of traditional

algorithms in processing nonlinear and non-stationary signals, significantly enhancing the identification accuracy and robustness of power quality disturbances. After analysis, the method proposed in this paper maintains fault diagnosis accuracy above 95% even under strong noise interference. Compared with traditional methods, including CNN and SVM, the accuracy can be improved by up to 5%. After optimization using the PSO algorithm, the model's accuracy increases by 3.6%, which demonstrates good applicability and robustness.

Specifically, the modified CEEMDAN approach successfully mitigates modal aliasing and spurious components, enabling a more precise decomposition of noisy signals into multiple IMFs, which lays a solid foundation for subsequent feature extraction. The introduction of HT further exploits the time–amplitude information and instantaneous frequency characteristics of the reconstructed signals, providing a rich and effective feature set for the classifier. Building upon this, the improved ELM is utilized as the classifier, leveraging its rapid learning speed and powerful nonlinear mapping capability to achieve precise identification of composite power quality disturbances.

Experimental results demonstrate that the proposed method not only excels in identifying various types of power quality disturbances but also maintains high accuracy even in noisy environments, fully validating its effectiveness and practicality in real-world applications. Furthermore, the method exhibits robustness and superiority in complex grid environments, offering potent technical support for power quality monitoring and management in modern power systems.

Author Contributions: Conceptualization, K.L., J.H., S.C., L.R., Y.L. and Y.W.; methodology, K.L., J.H., S.C., L.R., Y.L. and Y.W.; software, K.L., J.H., S.C., L.R., Y.L. and Y.W.; writing—original draft preparation, K.L., J.H., S.C., L.R., Y.L. and Y.W. All authors have read and agreed to the published version of the manuscript.

Funding: This research received no external funding.

Data Availability Statement: The data can be obtained by contacting the corresponding author.

Conflicts of Interest: Ke Liu, Jun Han and Yutong Liu were employed by Electric Power Research Institute of State Grid Qinghai Power Grid Corporation. The remaining authors declare that the research was conducted in the absence of any commercial or financial relationships that could be construed as a potential conflict of interest.

Nomenclature

Parameters and Variables	Meaning
$x(t)$	The original signal
$X(t)$	The signal with white noise added
ε_0	The amplitude coefficient of the white noise
$\omega_i(t)$	The white noise
$r_1(n)$	The residue component
$E_j(\cdot)$	The j-th order component
$r(n)$	The final residual component
N	The number of modal components generated
n	An index variable used to iterate through or index all data samples of the first intrinsic mode function
IMF_1^i	The intrinsic mode components obtained through CEEMDAN decomposition
$\sum_{j=1}^{k} IMF_j$	The signal IMF components
$\sum_{j=k+1}^{m} IMF_j$	The aliased IMF components

$\sum_{j=m+1}^{n} IMF_j$	The noise IMF components
$z(t)$	The random signal
$s(t)$	The complex-valued function
$a(t)$ and $\theta(t)$	The instantaneous amplitude and instantaneous phase
a_{ij}	The connection weight between the input layer and the hidden layer
o_j	The threshold of each hidden layer neuron
β_{ij}	The connection weight between the hidden layer and the output layer.
$g(x)$	The activation function of the hidden layer
H	The output matrix of the hidden layer
Y	The output matrix

References

1. Chen, J.; Zhao, Y.; Lin, H.; Wei, Y.; Liu, W.; Guo, Q.; Li, Y.R.; Mantooth, H.A. Analysis and Control of Cascaded Energy Storage System for Energy Efficiency and Power Quality Improvement in Electrified Railways. *IEEE Trans. Transp. Electrif.* **2024**, *10*, 1299–1313. [CrossRef]
2. Zhou, J.; Gao, Y.; Wu, C.; Gu, T.; Xu, C.; Lv, Q. Detection of Power Quality Disturbances Based on Improved Wavelet Threshold Function and CEEMD. *J. Electron. Meas. Instrum.* **2023**, *33*, 141–148.
3. Zu, L.; Liu, Z.; Sheng, N. Research on Denoising Method of Wavelet Transform under Non-stationary Acoustic Signals. *Mod. Electron. Technol.* **2022**, *45*, 35–40.
4. Zhang, Z.; Liu, M.; Yu, B.; Zhang, Z.; Wang, Q. Research on Denoising of Improved Wavelet Threshold New Algorithm in Power Grid Disturbance. *Mod. Electron. Technol.* **2024**, *44*, 53–57.
5. Boopathi, R.; Indragandhi, V. Experimental Investigations on Photovoltaic Interface Neutral Point Clamped Multilevel Inverter-Based Shunt Active Power Filter to Enhance Grid Power Quality. *IEEE Access* **2024**, *12*, 74482–74498. [CrossRef]
6. Monteiro, V.; Moreira, C.; Lopes, J.A.P.; Antunes, C.H.; Osório, G.J.; Catalão, J.P.S.; Afonso, J.L. A Novel Three-Phase Multiobjective Unified Power Quality Conditioner. *IEEE Trans. Ind. Electron.* **2024**, *71*, 59–70. [CrossRef]
7. Tang, F. Spectral Analysis of Interharmonics Based on Spatial Spectrum Estimation Algorithm. Master's Thesis, Lanzhou University of Technology, Lanzhou, China, 2022.
8. Grandke, T. Interpolation Algorithms for Discrete Fourier Transforms of Weighted Signals. *IEEE Trans. Instrum. Meas.* **2013**, *32*, 350–355. [CrossRef]
9. Harris, F.J. On the use of windows for harmonic analysis with the DFT. *Proc. IEEE* **1978**, *66*, 51–83. [CrossRef]
10. Ji, B.; Liang, Z.; Niu, S. FFT Harmonic Analysis Based on Nine-Term Cosine Combination Window with Minimum Sidelobes. *Electr. Power Sci. Eng.* **2022**, *28*, 16–21.
11. Wen, H.; Teng, Z.; Guo, S. Triangular Self-Convolution Window With Desirable Sidelobe Behaviors for Harmonic Analysis of Power System. *IEEE Trans. Instrum. Meas.* **2023**, *59*, 543–552. [CrossRef]
12. Luo, Y.; Li, K.; Li, L.; Huang, J.; Zhao, C.; Xiao, X. A Novel Recognition Method for Complex Power Quality Disturbances Based on Rotation Vector and Fuzzy Transfer Field. *IEEE Trans. Ind. Inform.* **2024**, *20*, 12502–12512. [CrossRef]
13. Shui, L.I.U.; Zhenxin, Z.H.O.N.G.; Ming, C.H.E.N.; Jiehuan, L.I.N.; Yang, Z.H.A.N.G.; Xianghua, P.E.N.G.; Jingyuan, Y.I.N. Power Quality Disturbance Detection Method Based on Improved Empirical Fourier Decomposition. *Mod. Electr. Power* **2023**, *40*, 465–473.
14. Sun, D.; Gao, Q.; Zhu, D.; Lu, Y. Adaptive Circular Power Harmonic Analysis Algorithm Based on Discrete Fourier Transform. *J. Anhui Univ. (Nat. Sci. Ed.)* **2023**, *37*, 57–64.
15. Hu, G.; Li, X.; Liang, D. Thin Cloud Removal from Remote Sensing Images Based on Dual-Tree Complex Wavelet Transform. *J. Anhui Univ. (Nat. Sci. Ed.)* **2024**, *40*, 50–58.
16. Li, B.; Cao, M.; Li, S.; Bao, W. Power Quality Disturbance Recognition Method Based on WT and GA-SVM. *Power Electron. Technol.* **2023**, *54*, 52–55.
17. Lopez-Ramirez, M.; Ledesma-Carrillo, L.; Cabal-Yepez, E.; Rodriguez-Donate, C.; Miranda-Vidales, H.; Garcia-Perez, A. EMD-based feature extraction for power quality disturbance classification using moments. *Energies* **2016**, *9*, 565. [CrossRef]
18. Cheng, Z.; Wu, J.; Liu, D.; Chen, L. Composite Power Quality Disturbance Detection Based on AMIST. *New Technol. Electr. Power Energy* **2020**, *39*, 59–65.
19. Yin, B.; He, Y.; Zhu, Y. A Method for Multi-Disturbance Detection and Recognition of Power Quality Based on Generalized S-Transform and Fuzzy SOM Network. *Proc. CSEE* **2023**, *35*, 866–872.

20. Fang, Y.; Pang, H.; Chen, Y. Detection Method of Voltage Sag Disturbance Based on Improved HHT. In *IOP Conference Series: Earth and Environmental Science, Volume 645, Proceedings of the 2020 International Conference on Smart Grid and Energy Engineering 13–15 November 2020, Guilin, China*; IOP Publishing Ltd.: Bristol, UK, 2021; p. 012069.
21. Tian, Z.; Fu, C. Localization and Classification of Power Quality Disturbances Based on HHT. *Power Syst. Prot. Control* **2023**, *43*, 36–42.
22. Xu, J.; Guo, T. Simulation Analysis of Power Quality Disturbance Detection Based on Improved HHT Combined with Improved S-Transform. *Autom. Technol. Appl.* **2024**, *37*, 98–102+109.
23. Sun, S.; Wang, Q.; Yan, H.; Lin, X.; Du, T. Application of EEMD in Power Harmonic Detection. *Proc. CSU-EPSA* **2024**, *28*, 25–31.
24. Xu, Y.C.; Gao, Y.K.; Li, Z.X.; Xi, L. Application of Improved LMD Algorithm in Power Quality Disturbance Signal Detection of Microgrid. *Power Syst. Technol.* **2019**, *43*, 332–341.
25. Dragomiretskiy, K.; Zosso, D. Variational Mode Decomposition. *IEEE Trans. Signal Process.* **2014**, *62*, 531–544. [CrossRef]
26. Xu, Y.; Gao, Y.; Li, Z.; Lu, M. Detection and Classification of Power Quality Disturbances in Distribution Network Based on VMD and DFA. *CSEE J. Power Energy Syst.* **2023**, *6*, 122–130.
27. Huang, C.; Zhou, T. A New Method for Power Quality Disturbance Detection Based on Variational Mode Decomposition. *Electr. Power Autom. Equip.* **2022**, *38*, 116–123.
28. Yu, K.; Jia, L.; Chen, Y.; Xu, W. The Past, Present and Future of Deep Learning. *J. Comput. Res. Dev.* **2013**, *50*, 1799–1804.
29. Valtierra-Rodriguez, M.; de Jesus Romero-Troncoso, R.; Osornio-Rios, R.A.; Garcia-Perez, A. Detection and Classification of Single and Combined Power Quality Disturbances Using Neural Networks. *IEEE Trans. Ind. Electron.* **2013**, *61*, 2473–2482. [CrossRef]
30. Dong, G.; Li, D.; Chen, Y.; Ma, X.; Fu, A.; Mu, G.; Xiao, B. Power Quality Disturbance Classification Method Based on Feature Fusion Parallel Optimization Model. *Proc. CSEE* **2023**, *43*, 1017–1027.
31. Ruan, J.; Jiang, H.; Li, X.; Shi, Y.; Chan, F.T.S.; Rao, W. A Granular GA-SVM Predictor for Big Data in Agricultural Cyber-Physical Systems. *IEEE Trans. Ind. Inform.* **2019**, *15*, 6510–6521. [CrossRef]
32. Wu, F.; Shi, G.; Wang, S. Inverse Kinematics Solution of Manipulator Based on PSO-ELM. In Proceedings of the 2019 IEEE International Conference on Cybernetics and Intelligent Systems (CIS) and IEEE Conference on Robotics, Automation and Mechatronics (RAM), Bangkok, Thailand, 18–20 November 2019; pp. 293–297.
33. Figueiredo, E.M.N.; Ludermir, T.B. Effect of the PSO Topologies on the Performance of the PSO-ELM. In Proceedings of the 2012 Brazilian Symposium on Neural Networks, Curitiba, Brazil, 20–25 October 2012; pp. 178–183.
34. Available online: https://download.csdn.net/download/ilovejohn/10338755?ops_request_misc=%257B%2522request%255Fid%2522%253A%25221b0063fc0b487f4f112ee63204460044%2522%252C%2522scm%2522%253A%252220140713.130102334.pc%255Fdownload.%2522%257D&request_id=1b0063fc0b487f4f112ee63204460044&biz_id=1&utm_medium=distribute.pc_search_result.none-task-download-2~download~first_rank_ecpm_v1~rank_v31_ecpm-3-10338755-null-null.269%5Ev2%5Econtrol&utm_term=IEEE33&spm=1018.2226.3001.4451.4 (accessed on 22 October 2024).

Disclaimer/Publisher's Note: The statements, opinions and data contained in all publications are solely those of the individual author(s) and contributor(s) and not of MDPI and/or the editor(s). MDPI and/or the editor(s) disclaim responsibility for any injury to people or property resulting from any ideas, methods, instructions or products referred to in the content.